Advanced Housing Materials for Extreme Space Applications

Linda Del Castillo, James P. Hoffman, and Gaj Birur
Jet Propulsion Laboratory, California Institute of Technology
4800 Oak Grove Drive
Pasadena, CA 91109
818-393-0418
Linda.DelCastillo@jpl.nasa.gov

Abstract—Thermal stresses have a significant impact on the mechanical integrity and performance of RF hybrid circuits. To minimize this impact, a series of spray deposited Si-Al alloys were evaluated for use in electronic housing applications. Current housings for RF modules in space-based applications are generally made from either Kovar or 6061 Al. Although Kovar has a coefficient of thermal expansion (CTE) close to those of GaAs and Si, it also possesses a 10x reduction in thermal conductivity and a 3x increase in density compared with those of 6061 Al. Although it provides improved heat dissipation properties, 6061 Al has a CTE that is nearly 4x that of Kovar. The controlled expansion (CE) spray deposited Si-Al housing materials discussed herein combine a CTE approaching that of Kovar, with a thermal conductivity approaching that of 6061 Al, and a density that is less than that of both materials. The mechanical behavior of select Si-Al alloys was evaluated along with the application of these materials for direct attachment of active devices. Assemblies were thermal cycled from -55 to +125°C.[1 2]

TABLE OF CONTENTS

1. INTRODUCTION

Active antenna arrays often possess large numbers of densely-packed, high-power, transmit/ receive (TR) modules. Thermal handling for these modules therefore becomes a critical component of the design. One method of effectively removing heat from high power devices is to directly attach them to high thermal conductivity housings that are connected to an effective heat sink. If the CTE of the housing is significantly higher than that of the device, environmental thermal cycling and power cycling can expose active devices within the TR modules to severe fatigue stresses. In addition, the high density of modules within the arrays requires that the mass per module be as low as possible.

This paper will discuss the evaluation of spray deposited Si-Al alloys for use within the electronic housing (chassis) as a means of minimizing the impact of thermal stresses. Current housings for RF modules in space-based applications are most often made from either Kovar or 6061 Al. Kovar is chosen based on its close CTE match with that of active devices (e.g. GaAs or InP) and ceramic substrates. Unfortunately, this material also has a thermal conductivity that is about an order of magnitude lower than that of Al, requiring intermediate Cu-Mo heat spreading carriers as an additional joint between active devices and the housing material. Also, the density of Kovar is over three times greater than that of Al. Although it provides improved heat dissipation properties, 6061 Al has a CTE that is nearly 4 times that of Kovar. The Si-Al alloys (CE7, CE9, CE11 and CE13) studied possess low CTEs (7-13ppm/°C), relatively high thermal conductivities (120-160 W/mK), and low densities (2.42-2.55 g/cc).

2. BACKGROUND ON CE ALLOYS

The series of controlled expansion (CE) bulk spray deposited Si-Al alloys evaluated herein were developed by Sandvik Osprey for electronic packaging applications. Compositions for the alloys evaluated are summarized in Table 1. The alloys contain trace amounts of Fe and Zr.

Table 1. CE Alloy Compositions

Alloy	Composition (wt.%)
CE7	70Si-30Al
CE9	60Si-40Al
CE11	50Si-50Al
CE13	42Si-58Al

A Si-Al phase diagram is provided in Figure 1.[1, 2] The two phases shown in the diagram are (Al), a face-centered cubic (FCC) phase containing 97.4% Al and 2.6%Si, as

[1] 978-1-4244-7351-9/11/$26.00 ©2011 IEEE.
[2] IEEEAC paper #1628, Version 2, Updated January 11, 2011

well as (Si), which contains 100% Si and exhibits a diamond structure. If processed using conventional ingot metallurgy, hypereutectic Al-Si alloys solidify with large columnar Si grains, which significantly impact the mechanical behavior of the alloys. Such characteristics are avoided in the CE alloys through the use of spray atomization and deposition processing.

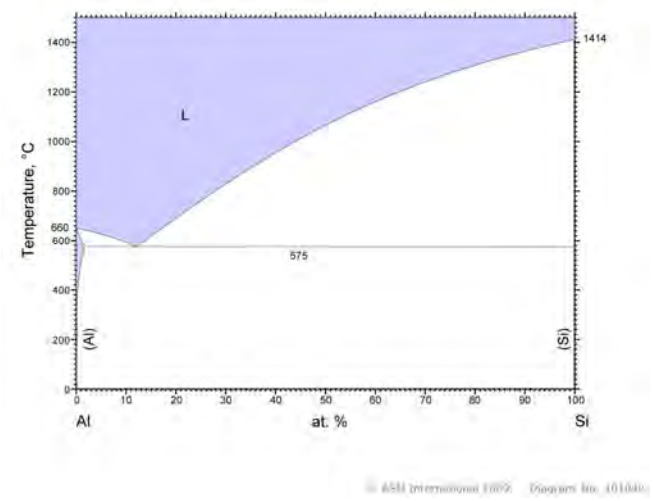

Figure 1. Binary Si-Al alloy phase diagram. [1, 2]

Spray Atomization and Deposition Processing

During spray deposition, the select alloy is inductively heated to well above the alloy melt temperature. The alloy is then transmitted through a nozzle and atomized using high velocity gas (N_2) jets. The semi-solid droplets then impact the substrate (initially) and eventually the rapidly solidified billet. The billets are then processed in a hot isostatic press. The resulting alloys are characterized by a fine, relatively isotropic grain structure with regions of Si-rich and Al-rich phases. [3]

4. MECHANICAL PROPERTIES

The tensile behavior of CE7, CE9, CE11, and CE13 was evaluated according to ASTM E8-04. Tests were performed using standard sub-size rectangular test specimens. Tensile results, provided in Figure 3, were compared with published data. As expected, strength increased with increasing Al contact. Tensile strength was highly dependent upon surface characteristics of the samples. The strain to failure was consistent with the expected characteristics of a brittle material. Fracture surfaces are shown in Figure 3, along with SEM and compositional analyses in Figures 4 and 5. The fine microstructure and relatively uniform distribution of Si and Al rich phases are clear in both figures for CE7 and CE9.

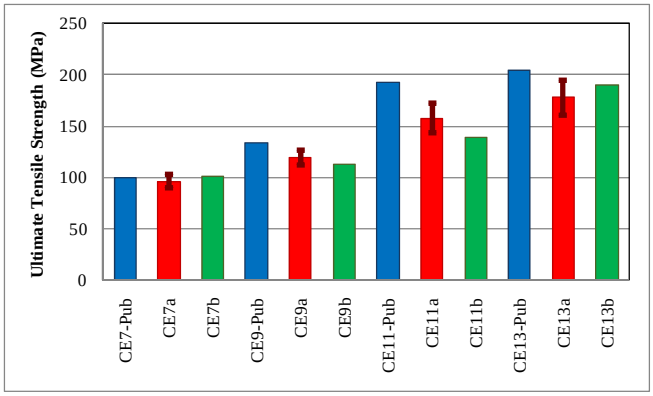

Fig. 2. Ultimate tensile strength for CE7, 9, 11, and 13. CEX-Pub refers to published data [4], CEXa refers to the average of all tensile tests performed for each material (including those that failed outside of the gauge section), and CEXb is the average of specimens that failed within the gauge section.

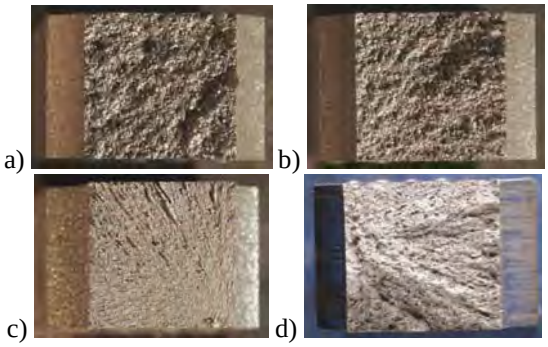

Figure 3. Optical fractographs of tensile tested samples for a) CE7, b) CE9, c) CE11, and d) CE13.

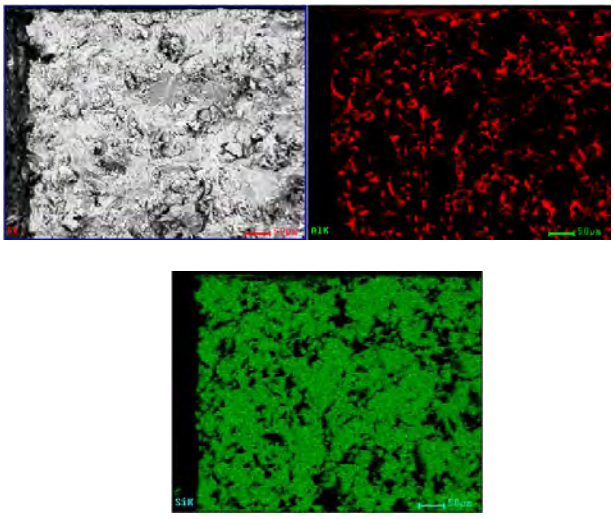

Figure 4. SEM fractograph and EDAX compositional images for the CE7 tensile fracture surface. Red and green indicate the presence of Al and Si, respectively.

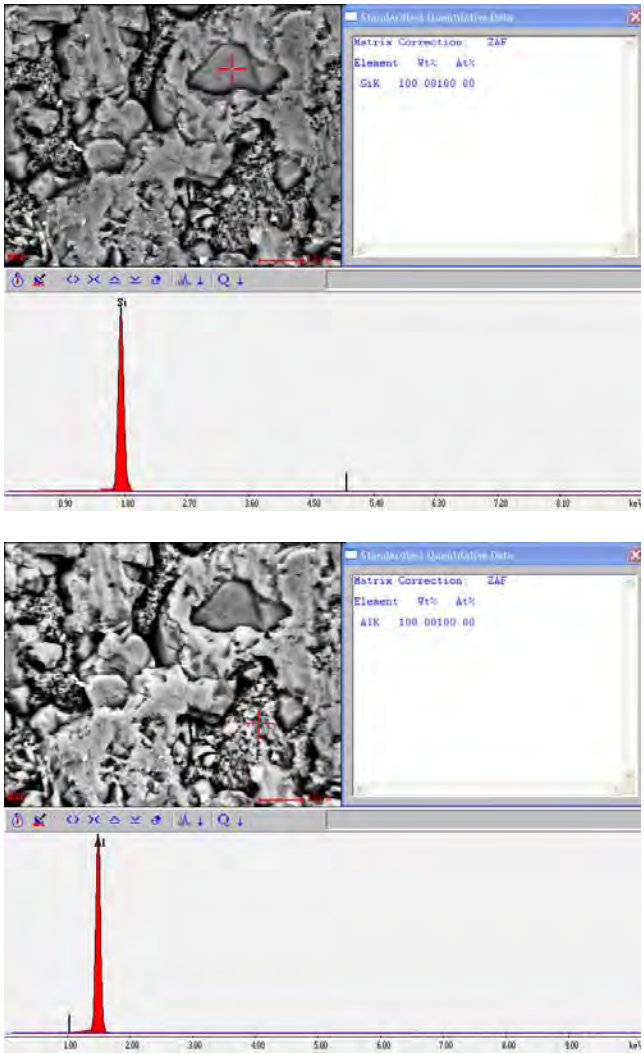

Figure 5. SEM fractograph and compositional analysis results for the CE9 alloy tensile fracture surface.

Four point bend tests were performed on CE7, CE9, CE11, and CE13 according to ASTM C1161-02c (08). Standard 90mm test specimens were machined from CE alloy plates in the as-received condition. Following machining, samples were ground to a fine finish in the longitudinal direction. The bend test results are provided in Figure 6. The bend strengths observed were higher than those provided in the published data.[4] As expected, specimens exhibited increasing flexural strength with increasing Al content. Failure was observed to be significantly influenced by surface finish and imperfections. A CE9 fracture surface obtained following bend testing in shown in Figure 7.

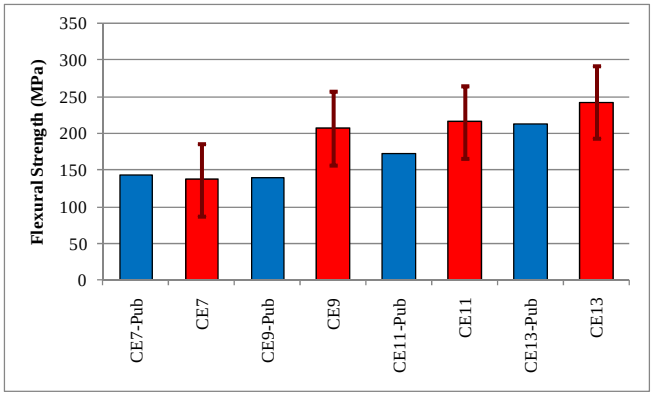

Figure 6. Flexural strength for CE7, CE9, CE11, and CE13. Experimental results were obtained using 4-point bend fixtures.

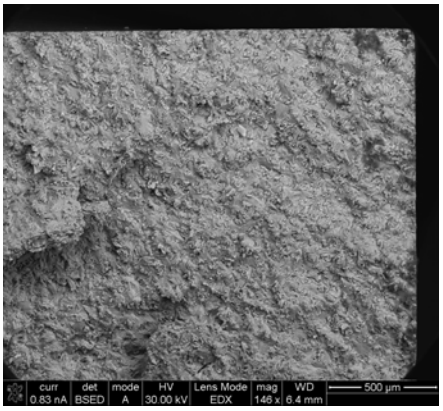

Figure 7. SEM micrograph of a fracture CE9 bend test sample.

5. Die Attach Studies

Due to the high Si content, the alloys exhibit low and stable CTEs, approaching those of Si, GaAs and InP active devices. Table 2 compares the CTEs of the four CE alloys studied with those of pertinent materials used in electronic packaging applications. A previous study on the reliability of GaAs solder attach to various substrates indicated that devices placed under compressive stress, as is the case with the high temperature solder attachment to substrates having a higher CTE than GaAs, did not degrade through life testing until the substrates exceeded a CTE of 16.5 ppm/°C.[5] Life testing for the current study included 1000 thermal cycles (-55 to 125°C). To verify the results of this study, GaAs mechanical die were attached to Ni/Au plated substrates of CE7, CE9, CE11, and CE13.

Table 2. CTEs of Various Relevant Electronic Packaging Materials

Material	CTE (ppm/°C) 25°C	Ref.
Al	23.6	[6]
Al_2O_3	6.7	[6]
CE7	7.2	[4]
CE9	9.1	[4]
CE11	11.4	[4]
CE13	12.2	[4]
Cu	16.6	[6]
GaAs	5.4-5.72	[6]
InP	4.5	[6]
Kovar	5.87	[6]
Mo	3.0-5.5	[6]
Si	2.3-4.7	[6]

The first set of substrates ordered exhibited blistering following exposure to the 80Au-20Sn reflow temperature (>280°C). It was determined that the Ni plating specified for these substrates (2.54-5.08 μm of electroplated Ni) and prebake temperatures were insufficient for the high soldering temperatures. Following discussions with Advanced Packaging Associates and Sandvik Osprey, it was determined that blistering issues could be minimized through the use of a higher prebake temperature and thicker electroless Ni plating. The reason for this modification was the fact that empirical evidence indicates a higher incidence of blistering when thinner nickel layers are subjected to higher temperatures. A second set of substrates was purchased with a Ni thickness of 10.16 μm and target soldering temperature of 325°C.

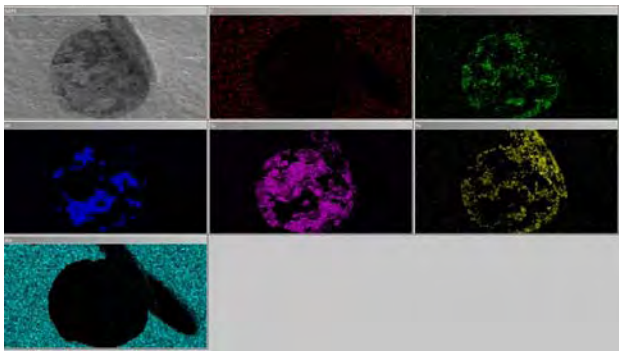

Figure 7. SEM secondary electron image and energy dispersive X-ray compositional analysis of a single blister on a plated CE9 substrate.

Upon receipt of the second set of substrates, the materials were heated to 325°C for 1 hour. Post exposure photographs are provided in Figure 8. No blistering was observed with the thicker Ni plating and the higher temperature plating pre-bake temperature.

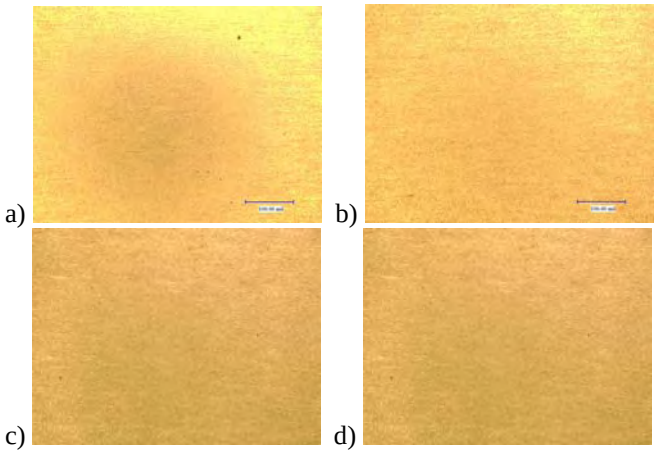

Figure 8. Optical micrographs of Ni/Au plated a) CE7, b) CE9, c) CE11, and d) CE13 substrates exposed to 325°C for 1 hour.

GaAs die were attached to each of the four materials using 80Au-20Sn solder at 300°C. Photographs of the complete assemblies are provided in Figure 9. The assemblies were exposed to 995 MIL-STD-883G Method 1010.8, condition B thermal cycles (-55 to 125°C) without failure.

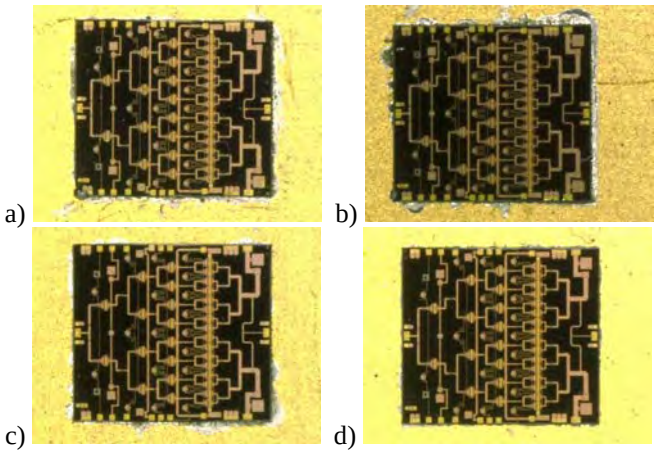

Figure 9. Optical micrographs of GaAs die attached to Ni/Au plated a) CE7, b) CE9, c) CE11, and d) CE13 following 790 thermal cycles.

6. RADIATION SHIELDING CHARACTERISTICS

No known evaluations on the radiation shielding characteristics of these materials have been published. The higher Al content alloys (such as CE13) are expected to have similar shielding behavior to that of Al. However, experimental evaluation of the higher Si content CE7 and CE9 would be useful to verify the shielding performance of these materials.

7. SUBSTRATE AND HOUSING APPLICATIONS

Osprey CE Alloys have become very useful in a variety of space based and terrestrial application. They have become an excellent choice for RF/microwave packages and carriers as well as heat sinks, optical and opto-electronic housings, carrier plates for laminate PCBs, guide bars for circuit boards, and fixtures in semiconductor processing equipment and soldering ovens.[7-8] An excellent report describing the evaluation of CE9 for ARTES 4 L & S Band Solid State Power Amplifier is provided in [9].

For the current evaluation, baseplates for a GaAs power amplifier circuit were machined from CE7 and CE11. Photographs of the two baseplates are provided in Figure 10. The circuits are currently being assembled onto the substrates and will be evaluated with respect to the electrical characteristics of the assembled circuits as a function of temperature.

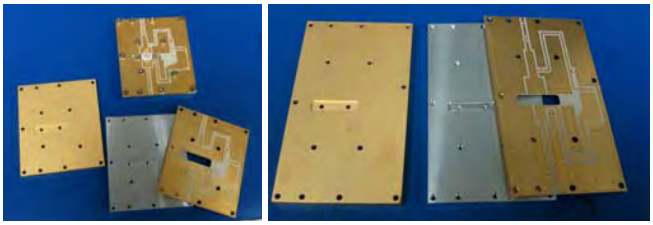

Figure 10. Photographs of RF evaluation carriers machined from CE7 and CE11.

8. SUMMARY

Four bulk, spray-deposited, controlled expansion Si-Al alloys were evaluated with respect to their mechanical behavior and thermal cycle reliability following attachment of GaAs die. It was found that materials exhibited sufficient strength for the target application. In addition, each of the materials studied exhibited excellent thermal cycle reliability following attachment to a GaAs power amplifier device. The improvement in mechanical behavior and ease of manufacturing for the various CE alloys indicate that alloy selection depends upon the level of deformation that the application can tolerate. For the present application, the most likely candidates for implementation are currently CE11 and CE13.

REFERENCES

[1] A.L.Udovskii, V.N.Karpushkin, and E.A.Kozodaeva, General algorithm, its mathematical basis and computer autonomic program for calculation of phase diagrams of binary systems, containing p disordered phases of variable and q phases of constant compositions at (p,q) ‹ 10, Calphad, Vol. 19, 1995, 245-277.

[2] P. Villars, editor-in-chief; H. Okamoto and K. Cenzual, section editors, ASM Alloy Phase Diagrams Center.

[3] S. P. S. Sangha, D. MI Jacobson, A. J. W. Ogilvy, M. Azema, A. Arun Junai and E. Botter, "Novel Aluminium-Silicon Alloys for Electronics Packaging," Engineering Science and Education Journal, 195-201, October 1997.

[4] Osprey Controlled Expansion Alloys Material Datasheets.

[5] J. Pavio and D. Hyde, "Effects of Coefficient of Thermal Expansion Mismatch on Solder Attached GaAs MMICs," IEEE MTT-S Digest, 1075-1078, 1991.

[6] M. G. Pecht, R. Agarwal, P. McCluskey, T. Dishongh, S. Javadpoir, and R. Mahajan, Electronic Packaging Materials and Their Properties, CRC Press, Boca Raton, FL, 1999.

[7] D.M. Jacobson, A.J.W. Ogilvy and A.G. Leatham, "Applications of Osprey Lightweight Controlled Expansion (CE) Alloys," 2005.

[8] D.M. Jacobson and A.J.W. Ogilvy, "Spray-Deposited Al-Si (Osprey CE) Alloys and their Properties," Materialwissenschaft und Werkstofftechnik, Volume 34, Issue 4, pages 381–384, April 2003

[9] S. Sangha, "Evaluation Report For Al-Si (CE9) Alloy for ARTES 4 L & S Band Solid State Power Amplifier," EADS Astrium Report A4W.RP.00002.DP.S.ASTR, Issue 02 Rev 00, 2006.

BIOGRAPHY

Linda Del Castillo *is a Senior Materials Scientist/Engineer in the Advanced Electronic Packaging Group at JPL. She received her B.S. in Mechanical Engineering from California State Polytechnic University, Pomona, followed by M.S. and Ph.D. degrees in Materials Science and Engineering from the University of California, Irvine. Since beginning her work at JPL in 2000, she has performed research on electronic packaging for active membrane radar applications, flexible embedded active devices, heterogeneous integration of a MEMS*

neuro-prosthetic system, MEMS fabrication, high voltage as well as high temperature/high frequency hybrid electronics and high temperature survivable electronic systems for the Venus environment.

***James Hoffman** is a Senior Engineer in the Radar Technology Development Group at JPL. He received his BSEE from the University of Buffalo, followed by MSEE and PhD from Georgia Tech in planetary remote sensing, and has worked in microwave instrument design for remote sensing applications for more than 10 years. In previous technology development tasks, he successfully developed a new low power digital chirp generator, which has been integrated into several radar flight instruments; he also designed, built and field tested the first tower radar for demonstration of active remote sensing of soil moisture. He is also the recipient of a NASA Tech Brief Award for his work in hybrid dual-channel Ka-band receivers, as well as for a single chip T/R module. He has experience designing radar systems for both technology development and space flight hardware development, and is currently the RF lead for the proposed DESDynI radar instrument.*

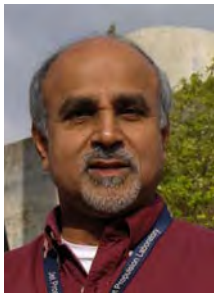

***Gaj Birur** is a Principal Engineer in the Mechanical Engineering Division at Jet Propulsion Laboratory, California Institute of Technology, Pasadena, California. He specializes in the areas of advanced spacecraft thermal control technologies and the design, build, testing of the planetary spacecraft missions. He has a Ph. D in mechanical engineering and has been working at JPL since 1979.*

ACKNOWLEDGEMENTS

The research described in this paper was carried out at the Jet Propulsion Laboratory, California Institute of Technology, under a contract with the National Aeronautics and Space Administration. The authors would like to thank Andrew Ogilvy from Sandvik Osprey Ltd as well as Stu Weinshanker and Jim Lawson from Advanced Packaging Associates for their help with this project.